Laser-Doppler Velocimeter Measurements in Simulated Entrained Gasifier Flows

A laser-Doppler velocimeter (LDV) was used in a cold-flow study of a simulated entrained-flow coal gasifier. The study was designed to provide fundamental information about the flows in such a gasifier and to provide data for the validation of a turbulence submodel used in modeling combustion processes. Measurements in 20 swirling and nonswirling flow cases were made with several levels of replication. This study emphasized the effects of inlet conditions on flow properties within the simulated reactor.

Unsteady flow phenomena with time scales on the order of seconds to minutes were sometimes observed. The unsteadiness was apparently associated with relaminarization-type flow transitions.

Comparisons were made with model predictions from PCGC-2, a model for combustion processes based on the $k - \epsilon$ turbulence model. Several areas of weakness in the model results were observed, but the unusual flow regimes measured in this study may be beyond the abilities of practical computer models.

Jeffrey D. Lindsay
Paul O. Hedman
Philip J. Smith
Department of Chemical Engineering
Brigham Young University
Provo, UT 84602

Introduction

Entrained-flow gasification of pulverized-coal has the potential to become a competitive source of energy. One near-commercial application is the use of an entrained-flow gasifier in an integrated gasification combined cycle (IGCC) (Clark and Shorter, 1986; Perry and Nager, 1986). In order to better understand and to improve pulverized-coal gasification processes, a large body of gasification data from within a laboratory-scale entrained-flow gasifier has been collected at this laboratory (e.g., Skinner et al., 1980; Soelberg et al., 1985; Hedman et al., 1985; Brown et al., 1986) and applied toward the development of a comprehensive computer model for pulverized-coal reactors (Smith et al., 1981; Smoot and Smith, 1985). This paper summarizes a companion LDV study of the flow processes in a simulated entrained-flow gasifier. Isothermal air flows were used to isolate the basic flow properties from such complications as density gradients and chemistry-turbulence interactions.

Emphasis was on the effects of inlet conditions on flow properties (e.g., axial velocity decay, location of recirculation zones, and turbulence). A knowledge of flow properties can lead to improved gasifier operating conditions, can assist in the interpretation of *in situ* chemical species data from the gasifier, and can guide modeling efforts. Validation of a specific computer model was also an objective of this study. The model, PCGC-2 (two-dimensional pulverized-coal gasification and combustion), is a comprehensive code for pulverized-coal and coal-water slurry processes (Smith et al., 1981; Smoot and Smith, 1985). The code employs the $k - \epsilon$ model for turbulent fluid mechanics.

Like the gasifier of this study, many combustion-related systems employ coaxial jets. The importance of such flows has led to many investigations of their behavior. Specific studies of note include those of Ribeiro and Whitelaw (1980), Claypole and Syred (1982), Roback and Johnson (1983), Mahmud et al. (1987), and Chigier and Dvorak (1975). Also, Gupta et al. (1984) and Sloan (1986) provide excellent reviews on the effects of swirl in such flows. Work directly related to coal combustion flows includes that of Webb and Hedman (1982) and Jones et al. (1984), who made LDV measurements of axial velocity in a cold, simulated pulverized-coal combustor flow. Intrusive probes were also used to study particle and gas mixing in several earlier studies of simulated pulverized-coal flows (Hedman et al., 1983; Tice et al., 1978).

The application of experimental data is crucial to the development and refinement of computer models. Model development has far outstripped the available data for comparison (Smoot and Hill, 1983). Much of the data from the past has been col-

Correspondance concerning this paper should be addressed to J. D. Lindsay, who is presently with The Institute of Paper Chemistry, Appleton, WI 54915.

lected with intrusive probes, which in some cases may seriously distort the flow being measured (Gouldin et al., 1983). Furthermore, most studies have not included measurements at the inlet. Documentation of the inlet boundary condition is often needed if experimental data are to be properly applied to model development (Sturgess, 1983).

The flow cases measured in this study help establish a database of use to the gasification studies in progress. One interesting finding was the presence of long-term, low-frequency transitions in some of the flow cases which seem to be related to relaminarization of the turbulent stream at low chamber Reynolds numbers. These transitions could not be related to changes in inlet or outlet conditions, and showed reproducible behavior. The relation between rms (root mean square) and mean velocities for multiple mean measurements in an unsteady zone appears to be consistent with the hypothesis of transitions between distinct metastable states. The possibility of transitions between metastable states for the geometry and flow rates of this study may explain some of the limitations in ability of the computer model to predict several details of the flow, especially the sensitivity to swirl in the secondary stream.

Experimental Approach

Experimental facility

A single-frequency backscatter-mode LDV system (TSI model 9100-6) with a 120-m W argon-ion laser was used in this study. All measurements were made with frequency shifting from a Bragg cell. Signals were processed with a counter (TSI model 1990A), and data sets from each measurement were stored on and reduced by an HP 1000 computer. A 'homemade' interface and signal driver system was used to multiplex and transmit the digital data to the computer across a 100-m distance.

The horizontal flow chamber used in this study simulates the cylindrical coal gasifier used for studies of reacting flow at this laboratory. Figure 1 shows the inlet configuration of the flow facility. The flow inlet consisted of an annular tube for the secondary stream (with annular diameters of 1.6 and 2.7 cm) around a central tube for the primary stream (ID 1.0 cm). The primary jet issued out of a pipe with a 3-mm-thick square lip which simulated the ceramic primary stream tube that was used in the reacting gasifier system of Soelberg (1985). A 35-degree half angle diverging nozzle, 4.0 cm in length, directed the streams into the 20-cm-diameter mixing chamber. The chamber was 90-cm-long and terminated with a conical contraction to a 13-cm-diameter pipe, through which the flow exited into the atmosphere. Swirl in the secondary stream was generated by a modified movable-block device (Beer and Chigier, 1972). The air in both streams was seeded with micron-sized alumina or titanium dioxide particles. Additional details are found in Lindsay (1986).

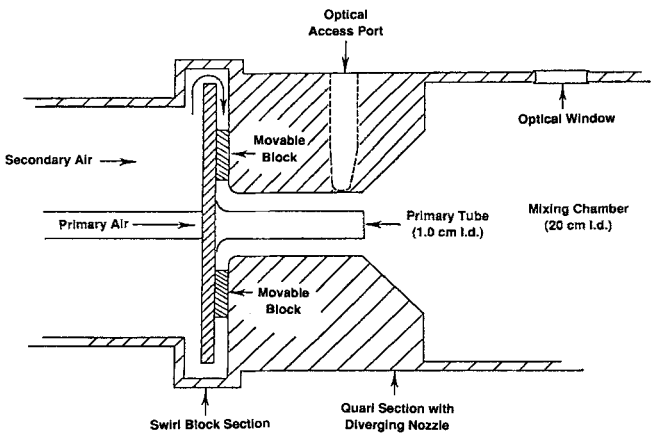

Figure 1. Inlet assembly in the cold flow facility.

Test program

LDV measurements were made in a variety of flow cases in order to observe the effects of different inlet conditions. A gasifier cold-flow case was specified by three inlet parameters: the mean primary stream inlet velocity, the mean secondary stream inlet velocity, and secondary swirl number. In this paper, a given flow case is designated with the notation $\langle Vp, Vs, S \rangle$, where Vp and Vs are the primary and secondary stream velocities, respectively, in m/s, and S is the secondary swirl number.

For the cases of most interest, primary and secondary inlet velocities were chosen so that inlet Reynolds numbers corresponded to those of Soelberg et al. (1985) for a reactive, entrained-flow, pulverized-coal gasifier. In these cold-flow cases, Vp was set at 34 ± 2 m/s, giving a primary stream Reynolds number of 19,000; and V_s was set at 5 ± 1 m/s, giving a secondary stream Reynolds number of 3,000 ± 600. The corresponding mean air mass flow rates at 20°C and 0.85 atm were 2.8 and 1.9 g/s, respectively. A factorial design for the test program was established, in which Vp had three levels (17, 34 and 51 m/s), V_s had three levels (0, 5 and 8 m/s), and S had three levels (0, 0.5 and 0.9). The test program required that axial and tangential velocity profiles be obtained at several axial stations for each flow case. Replicate measurements were also conducted.

With the above choices for inlet conditions, the amount of swirled flow from the secondary stream was not enough to induce central recirculation zones. (Some strongly-swirled flow cases were created by using swirled secondary flow only, but these were not of direct interest in this study.) The swirled flows, therefore, fall under the category of weakly swirling flows (Gupta et al., 1984). Under normal operating conditions, strong swirl is not possible in the actual BYU pulverized-coal gasifier.

Measurement techniques and bias correction

Initial work was done to ensure that acceptable measurement techniques would be used in the flows of interest. Theoretical considerations were combined with a series of LDV tests to establish criteria for settings of frequency shift, electronic filters, gain, and other electronic settings as a function of the local flow properties. Details on the settings used are given in Lindsay (1986).

Bias effects were of concern for the data rates and sampling procedures used in this study (Buchhave and George, 1979; Durao, 1980; Adams et al., 1986). Standard procedures to reduce bias effects include periodic sampling or random sampling with time-weighting of the mean and rms velocities (Durst et al., 1981). Time-weighting is frequently based on particle residence times or time-between-data values. Due to limitations of the 'homemade' interface system, the LDV system could not be operated in total burst mode, which precluded the measurement of true particle residence time in the probe volume (Adams et

al., 1986). Time-between-data values also could not be measured. Periodic sampling was not used and would have been impractical because of the generally low data rates encountered in this study.

An approximate time-weighted averaging method was employed, in which the weighing factor, t_i, is given by

$$t_i = \frac{N}{|f_s| + |f_d|} \tag{1}$$

where

N = number of Doppler cycles
f_s = frequency shift
f_d = pure Doppler shift due to the velocity of the moving particle

In total burst mode, this method would give results that would be independent of the frequency shift (Adams et al., 1986). In single burst mode, however, this weighing procedure is dependent on frequency shift. This was partially remedied through the use of special criteria for frequency shifting and for the averaging procedure (number-weighing vs. approximate time-weighing) as a function of the flow regime being measured. Low frequency shifts (0.01-1 MHz) were used for axial velocity measurements in the jet core regions, higher shifts (1-5 MHz) were used for axial velocity measurements in shear regions and recirculation zones, and high shifts (often 5-10 MHz) were used for tangential velocity measurements. Based on preliminary flow measurements and on a computational analysis of bias effects (Lindsay, 1986), approximate time-weighted averaging was chosen for axial velocity measurements in the core of the flow, where axial velocities were positive and dominant, and number-weighted averaging was generally used for tangential velocity measurements and for axial velocity measurements in the weak recirculation zones. The success of the bias correction procedure is evaluated below.

Results

Profile measurements

Measurements in 20 flow cases were made, 15 of which correspond to cases from the 3 × 3 × 3 factorial design. Table 1 lists the flow cases studied and the axial locations at which axial and tangential velocity measurements were made. Over 100 sets of useful velocity profile measurements were made, each with an average of 40 measurements at various radial locations. Profile measurements were made across most of the diameter of the flow chamber, partly in order to check flow symmetry. Replicate profile measurements (done on different days) were made to estimate the variance due to outside effects. Within each profile measurement series, replicate measurements at given points were also made to check experimental error and flow stability.

Sample mean and rms velocity profiles will be presented following a discussion of the observed unsteadiness and its implications.

Flow unsteadiness

While turbulent flows are truly transient, the flow properties averaged over a sufficient time can be highly reproducible. Many turbulent flows show this property which will be defined as "steadiness" in this paper. Since the turbulent time scale is often on the order of milliseconds, an averaging time of a few seconds is usually sufficient to observe steadiness. Since the LDV measurements of this study were averaged over 20 to 60 s, steadiness was expected. However, significant long-term unsteadiness was encountered in some cases. This behavior made the interpretation of the data more difficult.

It is believed that the unsteadiness is associated with the low chamber Reynolds numbers (500 to 2,500) in the mixing chamber for the flow cases of this study. While turbulence was indi-

Table 1. Measured Flow Cases*

Set	Case	Reynolds No. Primary ±5%	Reynolds No. Secondary ±10%	Axial Locations for Axial Vel. ±0.2 cm	Axial Locations for Tangential Vel. ±0.2 cm
1	⟨34,5,0⟩	19,000	3,000	*I*, 11, 20, 27, 43, 57	*I*, 11, 20, 27, 43
2	⟨34,5,0.5⟩	19,000	3,000	*I*, 11, 20, 27, 43	*I*, 11, 20, 27
3	⟨34,5,0.9⟩	19,000	3,000	*I*, 11, 20, 27, 43, 57	*I*, 11, 20, 27, 43
4	⟨34,0,0⟩	19,000	0	*I*, 11, 20, 27, 43	*I*, 20, 43
5	⟨51,7,0⟩	28,500	4,200	*I*, 11, 20, 57	*I*, 11, 20
6	⟨51,7,0.5⟩	28,500	4,200	*I*, 20, 27	*I*, 11, 20
7	⟨51,7,0.9⟩	28,500	4,200	*I*, 20, 57	*I*, 11, 20, 43
8	⟨51,0,0⟩	28,500	0	*I*, 11, 20, 43	*I*, 11, 20, 43
9	⟨17,5,0⟩	9,500	3,000	*I*, 11, 20	11, 20
10	⟨17,5,0.5⟩	9,500	3,000	11, 20	11, 20, 27
11	⟨17,5,0.9⟩	9,500	3,000	20	11, 20
12	⟨34,7,0.9⟩	19,000	3,000	11, 20	20
13	⟨34,7,0.5⟩	19,000	4,200		20
14	⟨51,5,0.5⟩	28,500	3,000		27
15	⟨51,5,0.9⟩	28,500	3,000		27
16	⟨0,5,0.5⟩	0	3,000		11
17	⟨0,5,0.9⟩	0	3,000		20, 27
18	⟨0,7,0.9⟩	0	3,000	20	20
19	⟨51,0,0⟩	28,500	0	11	
20	⟨60,0,0⟩	34,000	0	11	

*I designates measurements at the inlet plane. Flow cases are described by inlet primary velocity, secondary velocity, and swirl number, respectively, in brackets.

cated in all measurements, flow transitions associated with relaminarization (oscillations between metastable states) apparently occurred in the slower zones (away from the central core) of some flow cases.

Unsteady flow regimes were often encountered in low velocity regions beyond the 11- or 20-cm axial location. In such cases, successive LDV measurements at a single point showed fluctuations on the order of 10-100% in mean velocity values. However, fluctuations in the corresponding rms velocities rarely exceeded 10%. No simple periodicity was observed in the replicate LDV measurements. Unsteadiness was also observed for flow cases with primary flow only, and with primary and secondary flow together. The nature of the unsteadiness was reproducible: i.e., the degree of scatter and the relation between replicate mean and rms velocities could be reproduced.

Figure 2 shows sample time-series results from one of the simulated gasifier flows. The data were obtained with a hot-wire anemometer (TSI Air Velocity Meter, model 1650) placed on the centerline of an unsteady flow. The values shown are readings taken every 5 s and have effectively been averaged over approximately a 1-s period. Periods of steadiness, followed by large-scale unsteadiness, are evident. Similar behavior was observed in sequential LDV data.

Unsteadiness in the simulated gasifier flows was most severe in the swirled flow cases which became mixed more rapidly than the unswirled flows. A strong central jet in a poorly-mixed flow apparently stabilizes the flow, but as the axial velocity profile becomes flatter, transitions can occur. In strongly swirled flows with *central* recirculation zones, however, flow unsteadiness was not apparent, even when the chamber Reynolds number was as low as 500.

The possibility of low frequency fluctuations in the experimental system was examined and ruled out. An electronic control system, which regulated air flow from a large air tank, was initially suspected and was thus replaced with manual regulators having no possibility for dynamic oscillations. The observed unsteadiness could still be reproduced on different days and during different seasons of the year. Velocity measurements made at the inlet showed no unsteadiness; in fact, replicate mean axial velocity data for the inlet showed less variation than the data at any other axial location.

Following the simulated gasifier test series, the inlet geometry

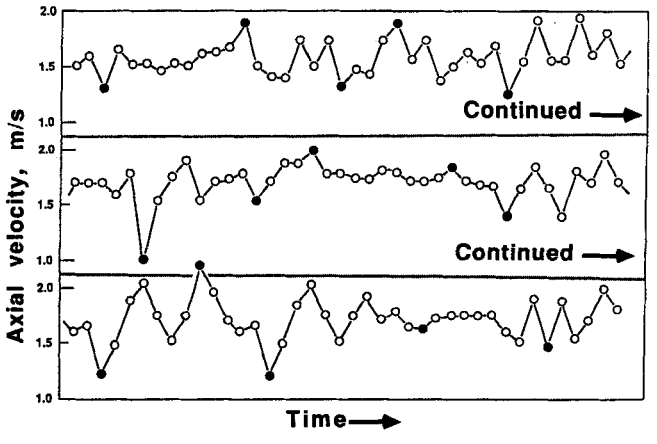

Figure 2. Sequential hot-wire anemometer data in an unsteady flow.
Velocities were averaged over roughly 1 s and recorded every 5 s.

of the flow facility was modified slightly to simulate the geometry and flows of the BYU pulverized-coal combustor. Measurements in the simulated combustor flows showed no unsteadiness at Reynolds numbers of 6,000 and higher. When the flows were reduced to give chamber Reynolds numbers in the 400–2,300 range, unsteady flows were again observed. The observed characteristics of flow unsteadiness in both reactor geometries are consistent with the hypothesis that large-scale flow transitions, possibly associated with partial relaminarization effects, are occurring in the low-Reynolds-number flows.

While they have not been thoroughly studied, relaminarizing flows have been observed in a variety of circumstances and can be found almost anywhere (Narasimha and Sreenivasan, 1979; Sreenivasan, 1982). Relaminarization can occur in three main situations:

1) In the expansion of a turbulent flow
2) In flows with curvature
3) In strongly accelerated flows

While most studies of relaminarization have dealt with the second and third categories, and thus are not applicable to the current study, Sibulkin (1962) studied the transition from initially turbulent to laminar flow in a pipe after a sudden expansion. The time-series behavior of the flow was apparently not examined, but the scatter in his mean velocity data may have been due to oscillations similar to those observed in this study.

Unsteadiness has been reported by other researchers. Hallet and Gunther (1984), for example, observed a low-frequency precession of a central jet about the flow axis in weakly swirled flows. Under some conditions the precession was irregular, with "the jet often pausing for a second or two on the axis before starting to precess again." Perry and Hausler (1982) observed unsteadiness in a plane jet flow. A variety of three-dimensional unsteady flow effects occur in strongly-swirled flows (Gupta et al., 1984; Sarpkaya, 1971).

Statistical analysis of unsteadiness

Under the assumption of flow oscillations between two well-defined states, the expected LDV results can be determined as a function of the time the flow spends in each state during the measurement. The expected mean is simply the time-weighted average of the two means. For large samples (many instantaneous velocity measurements), the expected rms velocity, $E(u')$, is given by

$$E(u') = (k\sigma_1^2 + (1 - k)\,\sigma_2^2 + k(1 - k)(U_1 - U_2)^2)^{1/2} \quad (1)$$

where k is the fraction of the time the flow is in State 1 during the LDV measurement, σ_1^2 and σ_2^2 are the variances of the velocity in States 1 and 2, respectively, and U_1 and U_2 are the velocity means of States 1 and 2, respectively. The measured mean velocity, U_m, is simply $kU_1 + (1 - k)U_2$. The relation between overall mean and rms velocities in the oscillating flow is then given by Eq. 1 after making the following substitution for k:

$$k = \frac{(U_m - U_2)}{(U_1 - U_2)} \quad (2)$$

The predicted relationship, $u' = f(U_m)$, is nonlinear with $\partial^2 u'/\partial U_m^2$ always negative. Depending on the range of values for k

encountered in a series of replicate measurements, the observed correlation curve (according to this model) may, however, appear to be nearly linear.

Using replicate LDV measurements at single locations in the unsteady flows, the correlations between means and rms velocity values at such points were examined. In the cases studied, the correlation coefficient (R value in a linear regression) could vary significantly with radial position. The effect of the observed flow transitions on the local mean and rms velocities is, therefore, complicated.

Figure 3 shows the correlation between successive mean and rms tangential velocities for LDV measurements at a point near the centerline (3.0 cm radial position) of an unsteady swirling flow with a chamber Reynolds number of 1,170. The inlet conditions include a primary stream Reynolds number of 9,500, a secondary stream Reynolds number of 3,000, and a secondary swirl number of 0.5. Measurements were made 27 cm downstream from the inlet. Multiple velocity measurements at this point were repeated on two different days. The maximum averaging time was 60 s, and the number of instantaneous velocity realizations per sample ranged from 700 to 3,000. A linear relationship between the mean and rms tangential velocity values can be seen. When linear regression is performed on all of the data, an R value of 0.95 is obtained ($R^2 = 0.90$). When the three rightmost points are assumed to be outliers and the data from the two runs are treated separately, the least square lines still have R values of 0.834 and 0.843, (corresponding to R^2 values of 0.696 and 0.712, respectively). In the latter case, the average correlation coefficient ($R = 0.839$) is large enough that the chance of such a correlation occurring purely by chance in a truly random case is less than 1%. The degree of correlation between mean and rms velocities may be interpreted as possible evidence for oscillations between metastable states. Data from other measurement sets with replications in unsteady flows also suggest the possibility of metastable states.

Using Eqs. 1 and 2, a predicted correlation curve is also shown on Figure 3, based on the assumption of two metastable states with average velocities of -0.4 and 0.6 m/s, and with rms velocities of 0.9 and 1.4 m/s, respectively. While the data are inadequate to specify the true flow properties of any possible metastable states, the predicted curve appears to be consistent with the data. This observation holds true with several other data sets

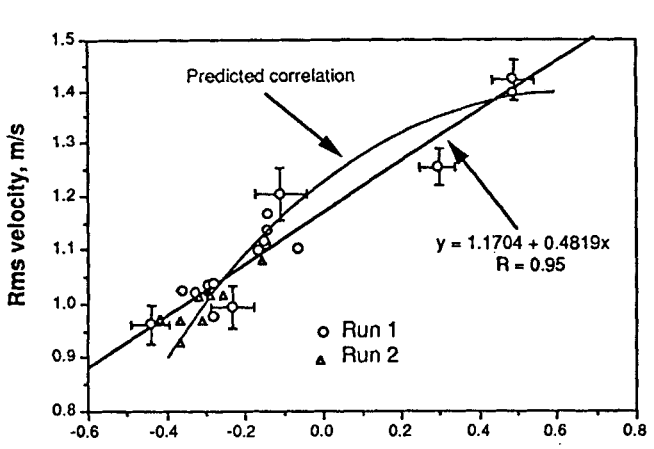

Figure 3. Correlation between replicate mean and rms LDV velocity measurements at a single point in an unsteady flow (Re = 1,170).

collected in unsteady flow regions, although the other sets lacked sufficient replications at single locations for conclusive examination of correlations. Details of the metastable states and of the transition mechanisms remain unknown, and further research into this largely unexplored area is needed.

The histograms of LDV velocity data taken in unsteady flows did not show bimodal distributions. Only when the difference between the means of two metastable states is significantly greater than their standard deviations (rms velocities), should a bimodal distribution be apparent in the histogram.

Sample profiles

Unsteadiness required that additional measurements be made at affected locations to determine time-averaged means. Several time-averaged velocity profiles are now presented. Radial profiles of mean axial and tangential, and rms axial and tangential velocity for case ⟨34,5,0.9⟩ are shown in Figures 4–7. Over 30 similar profile sets for other flow cases are given in Lindsay (1986). Vertical bars on the profiles show the range of replicate measurements at selected radial locations. Small numbers at the sides of the bars indicate how many duplicate measurements are included in each range. The range bars, roughly equivalent to 95% confidence bands for the mean flow, show the combined effect of experimental error, uncertainty due to flow unsteadiness and variance in profile duplications from different runs. The data in each range include measurements on both sides of the flow centerline, so any errors due to asymmetry are also included. The uncertainty at 95% confidence for individual mean velocity measurements is typically ± 0.2 m/s.

The axial velocity profiles in Figure 4 show that the coaxial jets merge into a single central jet which spreads and approaches the fully-developed state at the 57 cm location. Recirculating flow is present at all locations except possibly the last. (Measurements could not be made within 1 cm of the wall because of optical noise.) The magnitude of the maximum negative velocity changes only weakly with axial location. Significant unsteadiness in the flow was encountered at the 27-cm axial location, as is reflected in the large range bars.

The corresponding tangential velocity profiles in Figure 5 show a fairly rapid decay in tangential velocity as the axial velocity profiles flatten. The maximum tangential velocity of 3.5 ± 0.2 m/s at the inlet has decreased to a maximum of 0.2 ± 0.1 m/s after 27 cm.

Flow unsteadiness made determination of the tangential velocity profiles difficult. Unsteadiness was severe at the 11-27-cm axial locations, and is reflected in the large range bands for those velocity profiles. At the 27-cm axial location, such large fluctuations in tangential velocity were observed beyond about the 3.5 cm radial location that the profile shape in that region is unknown. The profile shape within 4 cm of the wall at the 20-cm axial location is also uncertain. Unsteadiness at the 43 cm axial location was also encountered, but was much less severe.

Examination of axial and tangential rms velocities in Figures 6 and 7, respectively, shows that the axial rms velocities are consistently higher. (An exception occurs at one radial location in the secondary inlet stream near the primary wall.) Both rms velocity components at the centerline increase rapidly from the low values at the inlet to values roughly three times as great at the 11-cm axial location. The profiles decay to fairly uniform values toward the end of the chamber. In the fully-developed primary inlet stream, the maximum rms velocities occur near

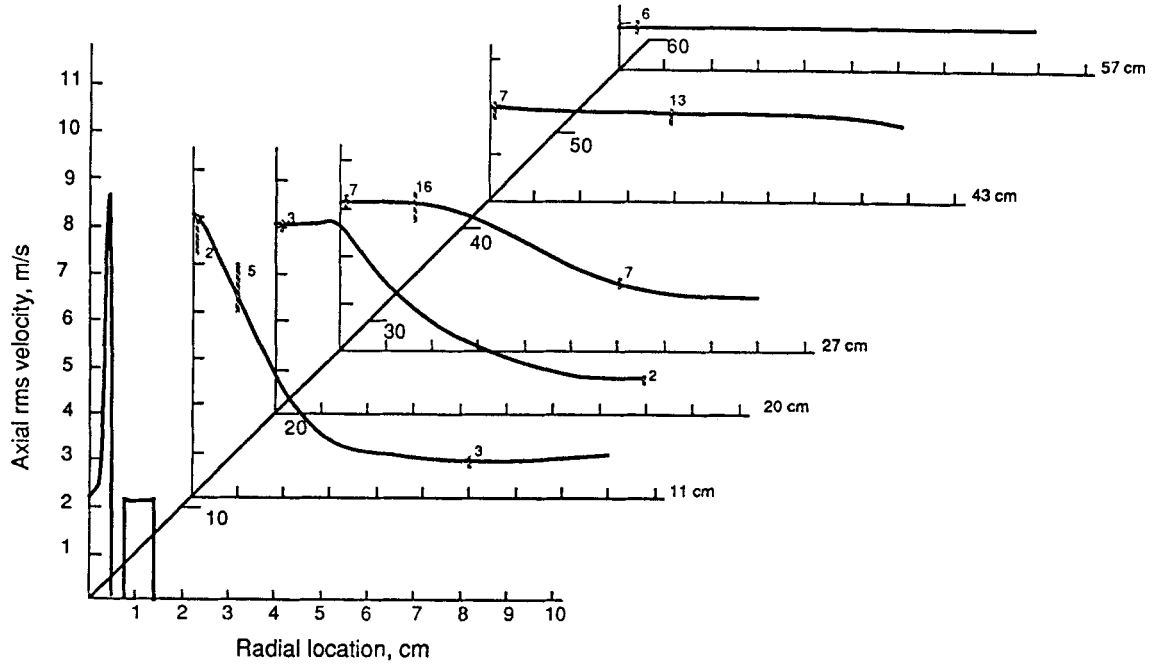

Figure 4. Axial velocity profiles for case ⟨34,5,0.9⟩.
Vertical bars show the range of data; numbers by the bars give the number of measurements in the range.

the wall. Once turbulent mixing occurs, the maximum rms velocity is at or near the centerline, with a minimum in the outer recirculation zone. A local maximum probably occurs near the chamber wall, but measurements could not be made close enough to the wall to observe these effects.

Unsteadiness in the flow had less effect on the rms velocity profiles than on the mean velocity profiles. Sources of variance other than unsteady flow largely contributed to the rms range bars (i.e., the range of replicate measurements within a single run was significantly less than the total range of measurements from all replicate runs). However, the range bars with 16 data points at the 27-cm axial location on Figure 6 and with 12 points at 11 cm on Figure 7 were due primarily to unsteady flow effects.

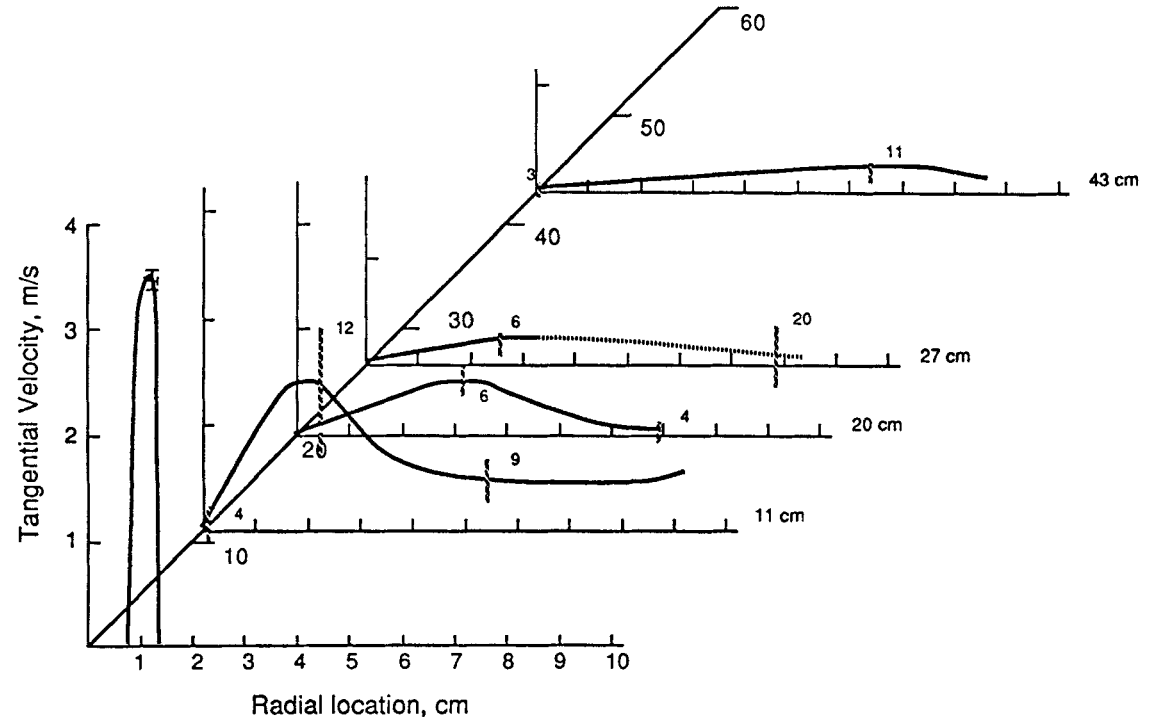

Figure 5. Tangential velocity profiles for case ⟨34,5,0.9⟩.
The dashed line at 27 cm indicates the assumed profile shape in a zone with serious unsteadiness.

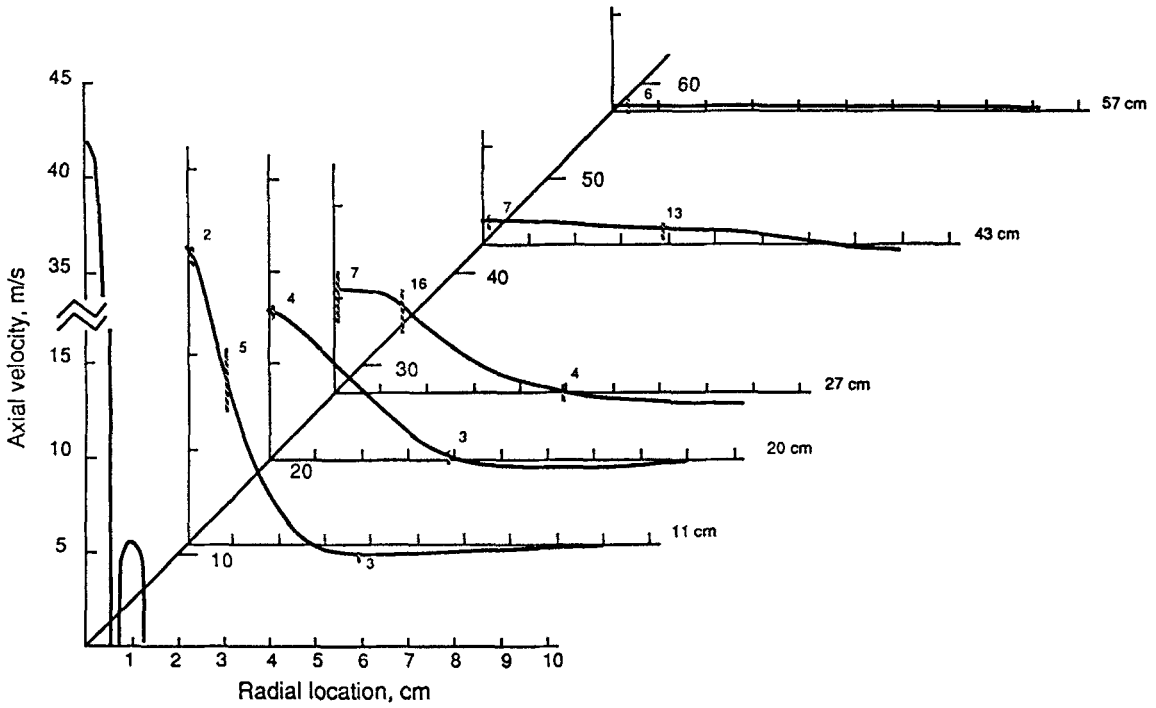

Figure 6. Axial rms velocity profiles for case ⟨34,5,0.9⟩.

Inlet measurements

Knowledge of the initial boundary conditions is often important if a body of data is to be applied to a predictive code. In some cases, the use of assumed inlet conditions can lead to serious errors in the predictions (Gouldin et al., 1983; Hendricks and Brighton, 1975). LDV measurements at the inlet plane were, therefore, included in this study.

A recessed optical access port was added in the inlet assembly after the downstream profile measurements had been completed. (See Figure 1.) In this way, a possible inlet perturbation, due to the presence of the port, did not affect the downstream measurements. The feed tube for the primary stream was located just upstream of the optical port, so that the laser beams would just miss the end of the pipe. This permitted inlet profile measurements to be made across both streams without addi-

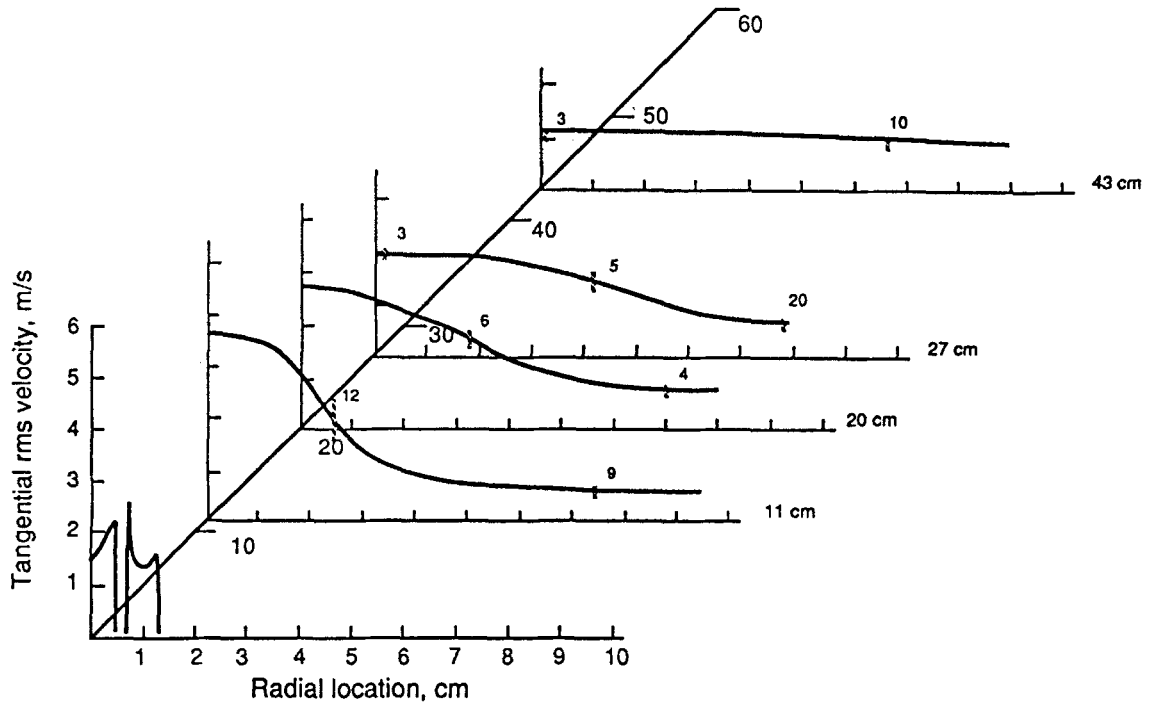

Figure 7. Tangential rms velocity profiles for case ⟨34,5,0.9⟩.

tional equipment modifications. These profiles were made only across one radial section, because scattered light from the remote secondary stream wall interfered with measurements made beyond the inlet centerline. It is recognized that the portion of the inlet flow in which these measurements were made may not correspond exactly to the flow at the beginning of the expanding nozzle, but no significant difference is expected to exist. For flow cases with primary flow only, the surrounding secondary duct and quarl section were removed to provide complete optical access to the primary jet.

Axial velocity profiles for the measured primary stream flows resembled typical profiles for fully-developed flow. Examples are shown in Figure 8, where mean and rms axial velocities for cases ⟨34,0,0⟩ and ⟨17,0,0⟩ are compared. The profiles are similar, differing by a scaling factor of 2. Axial velocity profiles in the secondary stream were affected by the swirl number, with swirl tending to flatten the profile.

The measured rms velocities (both axial and tangential components) across the primary inlet stream for all three levels of *Vp* agree well with other measurements in fully-developed pipe flow (Ribeiro and Whitelaw, 1980; Capp and George, 1982; Martin and Goucat, 1982). In Figure 8, for example, the expected high rms velocities, due to the pipe boundary layer, can be observed. Replicate inlet measurements showed no discernible differences in the rms profiles; and where symmetry could be examined (in the primary stream only), it was within 5%.

PCGC-2 predictions

A wide variety of predictions related to the simulated gasifier cold-flow tests were made with the PCGC-2 code (Smoot and Smith, 1985). Predictions of mean and rms velocities were compared with experimental data in order to evaluate the code. Comparisons were made for both centerline values along the axis of the flow chamber and for radial profiles at various axial locations. Unfortunately, because some of the flows of this study were complicated with long-term unsteadiness as described above, the applicability of the traditional $k - \epsilon$ model is in doubt. Nevertheless, some useful information can be obtained through examination of the modeling results.

In Figure 9, centerline values of axial velocity at various axial locations for several different flow cases are shown. These flow cases all have the same mean primary inlet velocity, 34 m/s. Examination of the experimental data shows the effects of swirl and secondary stream flow on the centerline axial velocities. For instance, comparison of data from case ⟨34,0,0⟩ (primary flow only) with case ⟨34,5,0⟩ (primary flow and unswirled secondary flow) shows that the secondary stream shields the central jet from the surrounding stagnant air and thus decreases the rate of axial velocity decay. The presence of swirl in the secondary stream (case ⟨34,5,0.9⟩), however, enhances mixing and causes a velocity decay rate greater than when no secondary stream flow is present.

A prediction from PCGC-2 made using standard theoretical inlet boundary conditions [1/7-power law, forced vortex in the secondary duct, eddy diffusivity inversely proportional to a length scale (details are given in Lindsay, 1986)] is also shown on Figure 9. The prediction for case ⟨34,5,0.9⟩ shows reasonable agreement with the corresponding data. However, the code predictions for the other experimental cases of Figure 9 are vir-

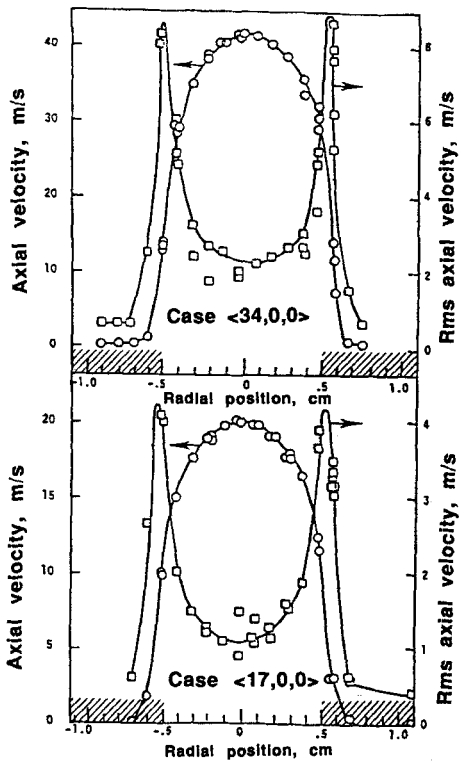

Figure 8. Mean and rms axial velocities at the inlet plane for cases ⟨34,0,0⟩ and ⟨17,0,0⟩.

Cross-hatching indicates the location of the primary tube wall.

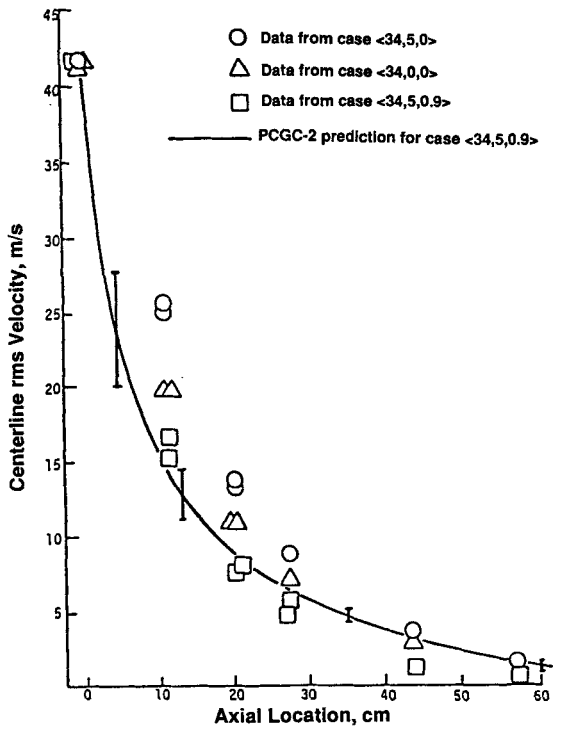

Figure 9. Measured and predicted centerline axial velocities for flow cases with 34 ± 2 m/s primary flow.

Vertical bars indicate ranges of PCGC-2 predictions with different grid densities and structures. 95% confidence intervals on data range from ±0.2 to 0.5 m/s.

tually the same as the prediction shown. The prediction for case ⟨34,0,0⟩, for instance, is only 0.7 m/s higher at the 27 cm location than the prediction shown in Figure 9, whereas the data show a difference of nearly 4 m/s at that location. The observed differences between the three experimental cases in the first 30 cm of the flow chamber are consistently much greater than the code predicts. Similar trends were observed for other flow cases. In general, the centerline axial velocity near the inlet is underpredicted, while the axial velocity further downstream (past roughly 30 cm) is overpredicted at the centerline. Increasing the grid resolution by 40% did not improve the predictions. Changing the grid structure to double the node density in the quarl section near the inlet also did not improve the predictions.

Because PCGC-2, like other $k - \epsilon$ models, has been successfully used in predicting a variety of flows in simple geometries (Rasband, 1988), the inability to accurately predict case ⟨34,0,0⟩ (a single jet expanding into the chamber) may be attributed to effects of the more complicated geometry of this flow or to the possible tendency to relaminarize in the chamber.

Figure 10 compares measured axial and tangential rms velocities along the chamber centerline for case ⟨34,5,0.9⟩ with the code prediction of tangential rms velocity. The prediction agrees well with the measured tangential velocity component. The predicted axial rms velocity curve is not shown, because it is nearly the same as the predicted tangential rms velocity curve. While the predicted axial rms values are always higher than the corresponding tangential predictions, the maximum difference is 8% at the peak in Figure 10 and approaches 0% at the inlet and outlet. The measurements show the axial rms velocity component to be consistently about 50% higher than the tangential component. This agrees well with other measurements in related flows (Capp and George, 1982; Champagne and Wygnaski, 1970). The model assumption of isotropic eddy diffusivity does not require the predicted rms velocities to be isotropic, but the predictions for case ⟨34,5,0.9⟩ are nearly isotropic, and in this respect compare poorly to the experimental data. Similar results were obtained with other flow cases.

Several factors may account for the failure of the model to predict the observed anisotropy in rms velocities. The $k - \epsilon$ model incorporates a linear relation between stresses and time-averaged velocities, following Jones and Launder (1972):

$$\bar{\rho}\,\overline{u_i' u_j'} = \frac{2}{3}\delta_{ij}(\bar{\rho}k + \mu_t \nabla \cdot \bar{\mathbf{U}}) - \mu_t(\nabla\bar{\mathbf{U}} + (\nabla\bar{\mathbf{U}})^T)_{ij} \qquad (3)$$

The turbulent viscosity is assumed to be isotropic, as is the eddy diffusivity. This does not force the normal stresses in Eq. 3 to be isotropic; but, if the velocity gradients are small, the right-hand side of Eq. 3 will be dominated by the turbulent kinetic energy, resulting in nearly isotropic rms velocities. A Reynolds stress model may be necessary to improve the predictions of rms velocity components. A second factor may be the low chamber Reynolds number typical of the cases in this study. The $k - \epsilon$ turbulence model may be inherently ill-suited for this difficult flow regime, as discussed below.

In addition to examining centerline conditions, direct comparison of measured and predicted radial profiles is also useful. In Figure 11, a predicted PCGC-2 velocity profile is compared with measurements for case ⟨34,0,0⟩ at the 27-cm axial location. Three sets of measurements made on different days have been compiled in this figure. The centerline axial velocity was underpredicted, although similarities in the observed and predicted profiles are evident.

Measured inlet conditions were used as code input in a number of predictions. Results were then compared to predictions made without the benefit of inlet data. Surprising agreement was found. For instance, superimposed plots of centerline axial velocity predictions for the two types of predictions were often indistinguishable. This is primarily because the assumed mean velocity inlet conditions used by PCGC-2 were close to the observed conditions, although that would certainly not always be the case. Probably of more importance is the small size of the inlet compared to the mixing chamber. The ratio of chamber to inlet cross-sectional areas is 55. Even when fine details in the small inlet can be represented with a limited number of nodes (typically 7–14 radial nodes for the inlet streams), they become relatively unimportant in the predictions past the large expansion. For the flows of this study, therefore, the use of experimental data for the inlet profiles did not appear to improve the accuracy of the predictions, although the data were useful as a check on the *a priori* inlet computations of PCGC-2.

Data accuracy and uncorrected bias effects

The intrinsic accuracy of the LDV system when measuring a steady, uniform Doppler shift was measured at ±0.2%. This includes the effects of optical misalignment, photodetector limitations, uncertainty in frequency shift and laser frequency, as well as errors in data acquisition and reduction. Measurements in real flows will have greater errors due to a variety of factors. The effect of random error on data accuracy was examined

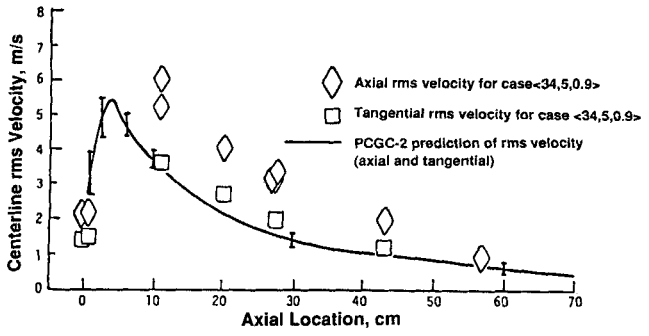

Figure 10. Measured and predicted centerline rms velocities for flow case ⟨34,5,0.9⟩.
95% confidence interval for data is ±7% or less.

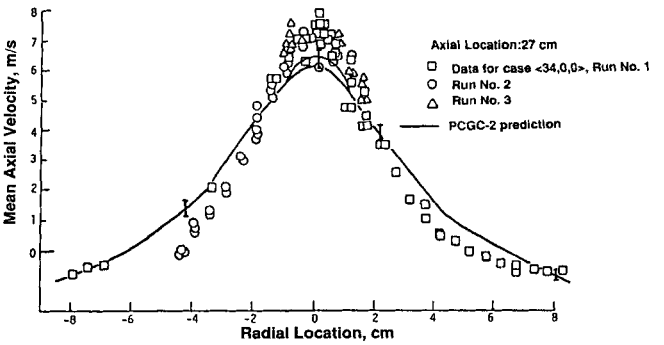

Figure 11. Measured and predicted axial velocities at the 27 cm location of flow case ⟨34,0,0⟩.

using replicate measurements. Replicate profile measurements from different runs (made on different days) gave centerline axial velocities which were, on the average, reproducible to within 6%. Errors in manually repositioning the LDV probe volume and variance in flow rates were the main sources of error in replicate profile measurements. In steady flow regions, the variance of replicate axial velocity measurements during a single run was typically about 1–3 times as great as the expected variance due solely to the effect of finite sample sizes.

Bias effects in turbulent flow can introduce serious systematic errors. The bias correction strategy of this study was limited in several respects and must be addressed. Examination of integrated mass balances from LDV data suggested that the negative velocities in some highly-turbulent recirculation zones (especially for the flow cases with 51 m/s inlet velocities) had magnitudes that were too great. In these recirculation zones, high frequency shifts (2–10 MHz) were required for axial velocity measurements; and for these shifts there was little difference between number-averaged and approximate time-weighted averaging. As a result, the higher number of fast moving particles passing through the probe volume per unit time may not have been adequately corrected in the averaging procedures.

The inadequately-corrected bias effects in these recirculation zone measurements were explored with computer simulation of LDV measurements in a stochastic three-dimensional flow field with mean and rms velocity components based on measurements (Lindsay, 1986). Lacking Reynolds stress measurements, the local instantaneous velocity components were assumed to be uncorrelated. Correction factors of 0.6 to 0.75 were computed for the negative velocities in the more turbulent cases where negative axial velocities as high as 1 m/s were measured. The correction factors estimated from the mass balance analysis ranged from 0.6 to 0.8 for the most turbulent cases and were near unity for the least turbulent flows with 21 m/s inlet velocities. These results indicate that the recirculation zone velocities in the more turbulent flow cases were too negative; this systematic error does not significantly alter the profile curves shown, because the absolute velocities in these zones were small compared to the rest of the flow.

Similar analyses of LDV bias effects suggest that bias was not an issue for the tangential velocity measurements nor for the axial velocity measurements in the positive regions of the flow. The limitations of the bias correction strategy due to the data acquisition system are nevertheless apparent, and an improved data acquisition system with better data sampling and bias correction capabilities has now been installed for future work.

Conclusions

A body of axial and tangential velocity measurements were made in cold flows in an entrained-flow gasifier geometry. The geometry consists of coaxial jets expanding in a quarl section followed by a sudden expansion into a cylindrical chamber. Of particular interest was the presence of very-low-frequency oscillations in the flow in a number of flow cases. The unsteadiness may have been caused by relaminarization-type flow transitions associated with the low Reynolds number in the flow chamber. In strongly swirled flows with central recirculation zones, however, flow unsteadiness was not apparent, even when the chamber Reynolds number was as low as 500.

Recirculating flow was present at most upstream locations. The magnitude of the maximum negative velocity changed only weakly with axial location. The corresponding tangential velocity profiles showed a fairly rapid decay in tangential velocity as the axial profiles flattened.

Axial rms velocities were generally higher than tangential rms velocities. Both rms velocity components at the centerline increased rapidly from the low values at the inlet to values roughly three times as great at the 11-cm axial location. The rms velocity profiles decayed to fairly uniform values toward the end of the chamber. In the fully-developed primary inlet stream, the maximum rms velocities occurred near the wall. Once turbulent mixing occurred, the maximum rms velocity was at or near the centerline, with a minimum in the outer recirculation zone. Unsteadiness in the flow had less effect on the rms velocity profiles than on the mean velocity profiles.

The use of assumed inlet conditions can lead to serious errors in the code predictions. Therefore, LDV measurements at the inlet plane were included in this study. Axial velocity profiles for the measured primary stream flows resembled typical profiles for fully-developed pipe flow. The measured rms velocities (both axial and tangential components) across the primary inlet stream for all the levels of primary jet velocity agreed well with other fully-developed pipe flow measurements.

The data were compared to predictions made by the fluid mechanics portion of the comprehensive combustion gasification model, PCGC-2. While predictions generally corresponded with the data, a major weakness in the predictions was the inability to predict the observed anisotropy in rms velocities. The model assumption of isotropic eddy diffusivity in the $k - \epsilon$ model may be the problem. Better predictions may require use of a Reynolds stress model. However, the presence of unsteadiness in many of the flows of this study may frustrate modeling attempts. Predictions also showed much less sensitivity to secondary swirl number than was observed, again possibly due to the complexity of unsteadiness in the flow.

For the flows of this study, little improvement in the predictions was possible through the use of measured inlet velocity profiles as code input, probably because the small dimensions of inlet area relative to the expansion chamber made small differences in inlet profiles relatively unimportant.

Acknowledgments

This research was supported by a National Science Foundation Graduate Fellowship and by the U.S. Dept. of Energy under contract DE-AC21-85MC22059 with Gary Friggens and Leland Paulson as the project officers during the study period. Lynda Richmond and Linda Ward provided secretarial and drafting support, and Mike King provided technical support on this study.

Literature Cited

Adams, E. W., J. K. Eaton, and J. P. Johnston, "An Examination of Velocity Bias in a Highly Turbulent Separated and Reattaching Flow," Symp. on Applications of Laser Anemometry to Fluid Mechanics, Lisbon, Portugal (July, 1984); *Laser Anemometry in Fluid Mechanics: II*, R. J. Adrian, D. F. G. Durst, H. Mishina, and J. H. Whitelaw, eds. Ladoan, Lisbon, Portugal (1986).

Beer, J. M., and N. A. Chigier, *Combustion Aerodynamics*, Applied Science, London (1972).

Brown, B. W., L. D. Smoot, and P. O. Hedman, "Effect of Coal Type on Entrained Gasification," *Fuel*, **65**, 673 (1986).

Buchhave, P., and W. K. George, Jr., "Bias Corrections in Turbulence Measurements by the Laser Doppler Anemometer," *Laser Velocimetry and Particle Sizing*, Proc. Int. Workshop on Laser Velocimetry, D. H. Thompson and W. H. Stevenson, eds., Hemisphere (1979).

Capp, S. P., and W. K. George, Jr., "Measurements in an Axisymmetric Jet Using a Two-Color LDA and Burst Processing," *Int. Symp.*

Applications of Laser-Doppler Anemometry to Fluid Mechanics, Lisbon, Portugal (1982).
Champagne, F. H., and I. J. Wygnaski, "An Experimental Investigation of Coaxial Turbulent Jets," *J. Heat Mass Trans.*, **14,** 1445 (1970).
Chigier, N. A., and K. Dvorak, "Laser Anemometer Measurements in Flames with Swirl," *Int. Symp. Combustion,* Combustion Institute, Pittsburgh, 573 (1975).
Clark, W. N., and V. R. Shorter, "Cool Water: Mid-term Performance Assessment," *EPRI Coal Gasification Contractor's Conf.* Palo Alto, CA (Oct. 15–16, 1986).
Claypole, T. C., and N. Syred, "The Stabilization of Flames in Swirl Combustors," *J. Inst. Energy,* **55,** 14 (1982).
Durao, D. F. G., I. Laker, and J. H. Whitelaw, "Bias Effects in Laser Doppler Anemometry," *J. Phys. E.: Sci. Inst.*, **13:** 442 (1980).
Durst, F., A. Melling, and J. H. Whitelaw, *Principles and Practices of Laser-Doppler Anemometry,* 2nd ed., Academic Press, New York (1981).
Gouldin, F. C., J. S. Depsky, and S. L. Lee, "Velocity Field Characteristics of a Swirling Flow Combustor," *AIAA Aerospace Sciences Meeting,* Reno, NV (Jan. 10–13, 1983).
Gupta, A. K., D. G. Lilley, and N. Syred, *Swirl Flows,* Abacus Press, Kent, England (1984).
Hallett, W. L. H., and R. Gunther, "Flow and Mixing in Swirling Flow in a Sudden Expansion," *Can. J. Chem. Eng.*, **62,** 149 (1984).
Hedman, P. O., D. R. Leavitt, and J. L. Sharp, "Cold Flow Mixing Rates in Confined, Recirculating Coaxial Jets with Angular Secondary Injection," *AIChE J.*, **31,** 1105 (1985).
Hedman, P. O., L. D. Smoot, T. H. Fletcher, P. J. Smith, and A. U. Blackham, "Prediction and Measurement of Entrained-Flow Coal Gasification Processes," Final Report, Combustion Laboratory, Chemical Engineering Dept., Brigham Young Univ., Provo, UT, USDOE Contract No. DE-AC21-81MC16518 (1985).
Hendricks, C. J., and J. A. Brighton, "The Prediction of Swirl and Inlet Turbulence Kinetic Energy Effects on Confined Jet Mixing," *J. Fluids Eng.*, **97,** 51 (1975).
Jones, W. P., and B. E. Launder, "The Prediction of Laminarisation with a Two-Equation Turbulence Model," *Int. J. Heat Mass Trans.*, **15,** 301 (1972).
Jones, P. G., J. L. Lindsay, and P. O. Hedman, "Fluid Dynamic Measurements in a Simulated Entrained-Flow Coal Combustor," Western States Section/Combustion Institute, Standard Univ. (Oct. 22–23, 1984).
Lilley, D. G., "Swirl Flows in Combustion," *AIAA J.*, **15,** 1063 (1977).
Lindsay, J. D., "LDA Measurements in a Simulated Gasifier with Swirl," Ph.D. Dissertation, Chemical Engineering Dept., Brigham Young Univ., Provo, UT (1986).
Mahmud, T., J. S. Truelove, and T. F. Wall, "Flow Characteristics of Swirling Coaxial Jets from Divergent Nozzles," *J. Fluids Eng.*, **109,** 275 (1987).
Martin, F., and P. Goucat, "Power Special Density of the Three Velocity Components in a Turbulent Flow at High Temperature," Int. Symp., *Applications of Laser-Doppler Anemometry to Fluid Mechanics,* Lisbon, Portugal (1982).
Narasimha, R., and K. R. Sreenivasan, "Relaminarization of Fluid Flows," *Advances in Applied Mechanics,* Chia-Shun Yih, ed., Academic Press, New York, **19,** 221 (1979).
Perry, J. H., and T. Hausler, "Aerodynamics of Burner Jets Observed for Brown Coal Fired Boilers," Report No. GO/83/57 for the Research and Development Department of the State Electricity Commission of Victoria, Australia (Dec. 1982).
Perry, R. T., and M. Nager, "Status of the Shell Coal Gasification Process," EPRI Coal Gasification Contractor's Conf., Palo Alto, CA (Oct. 15–16, 1986).
Rasband, M. W., "PCGC-2 and The Databook: A Concurrent Analysis of Data Reliability and Code Performance," MSc Thesis, Chemical Engineering Dept., Brigham Young Univ., Provo, UT (1988).
Ribeiro, M. M., and J. H. Whitelaw, "Coaxial Jets With and Without Swirl," *J. Fluid Mech.*, **96,** 769 (1980).
Roback, R., and B. V. Johnson, "Mass and Momentum Turbulent Transport Experiments with Confined Swirling Coaxial Jets," United Technologies Research Center, NASA Contract Report 168252 (Aug., 1983).
Sarpkaya, T., "On Stationary and Traveling Vortex Breakdowns," *J. Fluid Mech.*, **45,** 545 (1971).
Sibulkin, M., "Transition from Turbulent to Laminar Pipe Flow," *Phys. Fluids,* **5,** 280 (1962).
Skinner, F. D., L. D. Smoot, and P. O. Hedman, "Mixing and Gasification of Coal in an Entrained-Flow Gasifier," Paper No. 80-WA/HT-30, ASME Conf., Chicago (Nov., 1980).
Sloan, D. G., P. J. Smith, and L. D. Smoot, "Modeling of Swirl in Turbulent Flow Systems," *Prog. Energy Comb. Sci.*, **12,** 63 (1986).
Smith, P. J., T. H. Fletcher, and L. D. Smoot, "Model for Pulverized-Coal-Fired Reactors," *Int. Symp., Combustion,* The Combustion Institute, Pittsburgh, 1285 (1981).
Smoot, L. D., and S. C. Hill, "Critical Requirements in Combustion Research," *Prog. Energy Comb. Sci.*, **9,** 77 (1983).
Smoot, L. D., and P. J. Smith, *Coal Combustion and Gasification,* Plenum Press, New York (1985).
Soelberg, N. R., L. D. Smoot, and P. O. Hedman, "Entrained-Flow Gasification of Coal: 1. Mixing and Reaction Processes in an Entrained Coal Gasifier from Local Measurements," *Fuel,* **64,** 776 (1985).
Sreenivasan, K. R., "Laminarescent, Relaminarizing and Retransitional Flows," *Acta Mech.*, **44,** 1 (1982).
Sturgess, G. J., and S. A. Syed, "Calculation of Confined Swirling Flows," Paper 85-0060, AIAA Aerospace Sciences Mtg., Reno, NV (Jan. 14–17, 1985).
Sturgess, G. J., S. A. Syed, and K. R. McManus, "Importance of Inlet Boundary Conditions for Numerical Simulation of Combustor Flows," Paper 83-1263, Joint Propulsion Conf., Seattle, WA (June 27–29, 1983).
Tice, C. L., and L. D. Smoot, "Cold Flow Mixing Rates with Recirculation for Pulverized-Coal Reactors," *AIChE J.*, **24,** 1029 (1978).

Manuscript received Sept. 16, 1988, and revision received May 12, 1989.